J. Materials, Conc. Struct., Pavements, JSCE, No.648／V-47, 253-264, 2000 May

ANALYSIS OF SHEAR FAILURE IN R.C. BEAMS CONSIDERING LOCALIZATION PHENOMENON

Mohammad Reza SALAMY [1], Guoxiong YU [2] and Tada-aki TANABE [3]

[1] Member of JSCE, Graduate student, Dept. of Civil Eng., Nagoya University (Furo cho 1, Chikusa ku, Nagoya 464-8603, Japan)

[2] Member of JSCE, Dr. of Eng., Oriental Co. (Meieki 4-27-20, Nakamura-ku, Nagoya 450-0002, Japan)

[3] Fellow of JSCE, Dr. of Eng., Professor, Dept. of Civil Eng., Nagoya University

A method has been used to simulate shear failure in reinforced concrete elements considering localization phenomenon. This paper is dedicated to the modeling of the shear band localization in context of large strain accumulation in a narrow band without substantially affecting the strain in the surrounding material. This phenomenon frequently occurs accompanying inelastic deformation and material acoustic tensor looses its positive definiteness. Furthermore, finite element method is used to simulate this phenomenon. The model, when used in finite element context, gives mesh-insensitive results regarding to the width and direction of the shear band.

***Key Words** : localization phenomenon, bifurcation, shear failure, shear band, finite element method.*

1. INTRODUCTION

Mechanism of shear failure in concrete as well as reinforced concrete has been a long-standing key problem that is not fully clarified and should be argued from various angles. Experiments show that in close vicinity to the peak point, before or after that a localized damage band could often be observed in reinforced concrete structures. For some kinds of structures like heavily reinforced shear wall, concrete crack occurs firstly at the early stage of loading. However as the external load increases to the certain extent, a damage band would occur within a short interval of time along the direction which is entirely different from the initially formed crack direction. But in the case of reinforced concrete beams, regarding to the amount of longitudinal bars and also web reinforcement, damage band direction usually is near to initially formed crack direction.

The analysis of localization phenomenon in shear walls has been successfully carried out in Nagoya university[1]. In the reinforced shear walls, two modes of failure have been observed. For mode I, the ultimate failure occurred with the yielding of reinforcements and actually the damage seemed not so localized. In the case of mode II, the ultimate failure occurred with a shear band always formed parallel to one of the edges of the specimen. Once this phenomenon occurred, the structure would fail with large strain localizing inside the damage band without affecting the other parts of the structure. For this kind of failure, the peak point of loading and also the post peak behavior can not be obtained correctly by analysis without knowing what is the reason for this phenomenon and how to simulate this phenomenon by numerical analysis.

So far the continuos model is always adopted to explain the shear failure using softening shear modulus in the inclined crack surfaces[2]. However in these analyses, the existence of the point where the determinant of localization tensor passes zero value is never checked. In other words, they simply neglected those points even if they may exist. On the other hand according to Hill[3], a shear band is considered as a thin material layer that is bounded by two material discontinuity surfaces of the velocity gradient. A major motivation to determine analytically the critical bifurcation directions is the interest in localization phenomenon that has been displayed in recent years in the context of finite element analysis. To capture localized deformation patterns along the characteristics, the element mesh may be designed accordingly or enriched with the special shape function as described by Ortiz *et al.*[4]

This localization condition describes the formation of a discontinuity in the field of velocity gradients across a surface defined by the normal vector $\mathbf{n}$. Discontinuous bifurcation is signaled by a singularity of the acoustic or localization tensor $\mathbf{A(n)}$ when *det* $\mathbf{A(n)}=0$.

The main objective of this paper is to follow the

localization criteria and to present the embedded crack representation for reinforced concrete members which failed in either tension or shear. In this approach, a crack is modeled as a discontinuity within an element. This has the advantage of avoiding the implementation complexities of discrete crack models. The crack is regarded as a jump in displacements (Ortiz *et al.*, 1987) or the displacement gradients (Belytschko *et al.*, 1988). This jump functions can be added to the standard shape functions of the finite element. In the discontinuity element, a length scale parameter is introduced which is a material parameter and can be related to the size of the fracture process zone. This parameter solves the mesh-size dependence problem as present when a standard crack model is used. In this algorithm, *sub-h* producer relative to the localization bandwidth *b* has been used. In *sub-h* approaches the localization bandwidth is smaller than mesh size *h*, which in *super-h* approaches the localization band is larger than an element size.

In this paper, the analysis is concentrated to reinforced concrete elements subjected to uniaxial loading and also beams with or without web reinforcement which all of them failed in shear as reported in the experiment results. First, some theoretical aspect of localization formulation with embedded localization zone and strain jumping are scrutinized. Then the finite element formulation with embedded localized band is used to simulate this phenomenon in reinforced concrete structures. In the next part, constitutive models in both tension and compression will be explained. Finally, uniaxial case and also analytical results comparing with experiments show the capability of this method to simulate shear failure in reinforced concrete beams.

2. LOCALIZED FAILURE

In this part we review some theoretical aspects of the localization phenomenon and mathematical formulation used in finite element method. Localization is a phenomenon that large strain accumulates inside a part of material without substantially affecting the strain in the surrounding materials.

As mentioned, localization usually takes place when acoustic tensor ceases to be positive definite. To derive under what condition this kind of localization will be triggered, we will adopt the element level bifurcation analysis of Ortiz, *et al.*[4] which is based on the stationary acceleration wave analysis of Hill [3]. The physical mechanism for this phenomenon is that strain field across the damage band can possibly takes a jump, while the

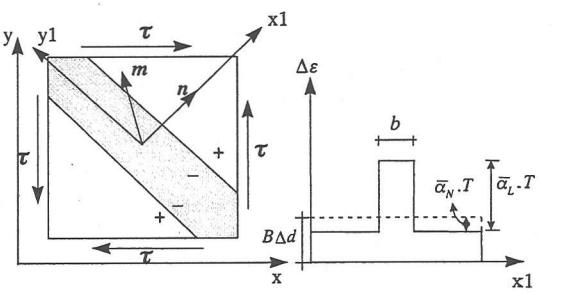

Fig. 1 Localize damage band and strain jump

equilibrium of the stress across the damage band remains to be satisfied (**Fig.1**). However, it is notable that the theory also can be applied for the composite materials such as reinforced concrete elements.

The incremental stress-strain relation can be put in the form

$$\dot{\sigma}_{ij} = D_{ijkl}\dot{\varepsilon}_{kl} \tag{1}$$

where D_{ijkl} is the tangential constitutive matrix of the material. For plastic solids, **D** has two branches, corresponding to plastic loading and elastic unloading respectively. Taking jump of (1) gives

$$\left\|\dot{\sigma}_{ij}\right\| = D_{ijkl}\left\|\dot{\varepsilon}_{kl}\right\| \tag{2}$$

The notation $\| \ \|$ means the differences values across the discontinuous surface($\|\sigma\| = \sigma^+ - \sigma^-$, see also **Fig.1**). Equilibrium across discontinuity planes requires that traction *t* be continuous then

$$\left\|\dot{t}_j\right\| = \left\|n_i\dot{\sigma}_{ij}\right\| = 0 \tag{3}$$

where **n** is the normal to the incipient plane of discontinuity. Combining (2), (3)

$$n_i D_{ijkl}\left\|\dot{\varepsilon}_{kl}\right\| = 0 \tag{4}$$

Compatibility requires that a jump be of the form

$$\left\|u_{i,j}\right\| = u^+{}_{i,j} - u^-{}_{i,j} = g_i n_j \tag{5}$$

where the superscripts 'plus' and 'minus' refer to the two sides of the plane of discontinuity, regarded as an oriented surface (**Fig.1**), and g_i are arbitrary. For the vector **g** it proves convenient to introduce the unit vector

$$m_i = g_i / g \ , \quad g = |\mathbf{g}| \tag{6}$$

Likewise, the strain field exhibits a jump of the form

$$\left\|\varepsilon_{ij}\right\| = \frac{1}{2}(m_i n_j + m_j n_i)g \tag{7}$$

Substituting (7) into (4) gives

$$A_{jk}(\mathbf{n})m_k = \left(n_i D_{ijkl} n_l\right)m_k = 0 \tag{8}$$

Clearly, equation (8) requires that

$$det(\mathbf{A}(\mathbf{n})) = 0 \tag{9}$$

Thus, a necessary condition for localization is that equation (9) has solution $\mathbf{n}$ (see Appendix A). Such solutions determine the normal to the possible planes of strain discontinuity. The geometry of the localized mode is fully determined by $\mathbf{n}$ and corresponding zero eigenvectors $\mathbf{m}$ of the acoustic tensor (8). If the material satisfies equation (8), then increments of strains can have a jump along the discontinuous surface (**Fig.1**) and is given by:

$$\left\|\Delta\varepsilon\right\| = \Delta\varepsilon^{+} - \Delta\varepsilon^{-} = \alpha\hat{\mathbf{T}} \tag{10}$$

where in two dimensions

$$\hat{\mathbf{T}} = \begin{bmatrix} m_1 n_1 \\ m_2 n_2 \\ m_1 n_2 + m_2 n_1 \end{bmatrix}, \varepsilon = \begin{Bmatrix} \varepsilon_x \\ \varepsilon_y \\ 2\varepsilon_{xy} \end{Bmatrix} \tag{11}$$

then

$$\left\|\Delta\varepsilon\right\| = \alpha(m_1 n_1, m_2 n_2, m_1 n_2 + m_2 n_1)^T \tag{12}$$

where α is the strength of the jump mode $\hat{\mathbf{T}}$ while the equilibrium across the discontinuous planes remains to be satisfied. In the local coordinate system $x_1 - y_1$, that is

$$\left\|\Delta\sigma\right\| = (\Delta\sigma_{x1}, \Delta\sigma_{y1}, \Delta\tau_{x1y1})^T = (0, \Delta\sigma_{y1}, 0)^T \tag{13}$$

This model of calculation takes advantage of the fact that considerable information concerning the localization process can be readily obtained at the element level. The method aims at utilizing this information to enhance the performance of the element in the presence of localized failure. It is of interest that Eqs. (7) and (10) give the same amount for g and α as the strength of the jump in strain field but α will be divided to α_L and α_P which are given in the next section.

It is notable that $\mathbf{n}^T\mathbf{m}$ can define the type of the failure. For a pure mode-I, $\mathbf{m}$ is aligned with $\mathbf{n}$ and $\mathbf{n}^T\mathbf{m} = 1$, on the other hand for a pure mode-II, $\mathbf{m}$ is perpendicular to $\mathbf{n}$ then $\mathbf{n}^T\mathbf{m} = 0$. Alternatively the first condition is related to the tension failure and the second one indicates shear failure likewise between two amounts is possible which shows mixed mode of failure in the element.

To add reinforcement effects to the model we can use tangential constitutive matrix for the composite material $\mathbf{D}_{RC}$ with or without bond effect between reinforcement and its surrounding concrete. The model was developed in Nagoya University with considering bond effect in the context of crack strain[6]. In this paper for the sake of the simplicity, we assumed that bond effect is perfect in the sense of smeared evaluation of strains. Then tangential constitutive matrix can be obtain simply as:

$$\mathbf{D} = \mathbf{D}_{RC} = \mathbf{D}_S + \mathbf{D}_C \tag{14}$$

where $\mathbf{D}_C$ and $\mathbf{D}_S$ are tangential constitutive matrix for concrete and reinforcement respectively. Note that in this paper, tangential constitutive matrix for the composite material $\mathbf{D}_{RC}$ is used in equation (4) in the following analysis.

3. FINITE ELEMENT FORMULATION

In the previous part, some aspect of localized failure has been clarified. Herein, finite element formulation for the so-called embedded localization zone is presented to follow post bifurcated behavior. Using the nomenclature of Belytschko *et al.*, we conclude from the literature that most strategies that have been suggested for resolving the nature (direction and width) of the localized zone are of type *iso-h,* such as enrichment of the element approximation with shape functions that present strain discontinuity within the element interior, or mesh realignment strategy that allows for strain discontinuities only along inter-element boundaries. Strategies to obtain 'mesh objectivity' with respect to energy dissipation for given h, when the softening behavior is a result of tensile cracking, also belong to the *iso-h* category [7].

Approaches type *sub-h* are those which employ shear bands embedded in elements. An appealing property of *sub-h* techniques is that bandwidth of localized zone b becomes independent of mesh size h as long as requirement $b<h$ is satisfied.

In order to take a factor of localization into consideration, the finite element with embedded discontinuous displacement field was used (Belytschko, T. *et al.*[5]). In the absence of localization, the strain increment is defined by $\Delta\varepsilon = \mathbf{B}\Delta\mathbf{d}$ (**Fig.1**), where $\Delta\mathbf{d}$ is the increment of

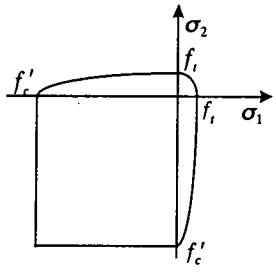

Fig. 2a Failure surface for concrete

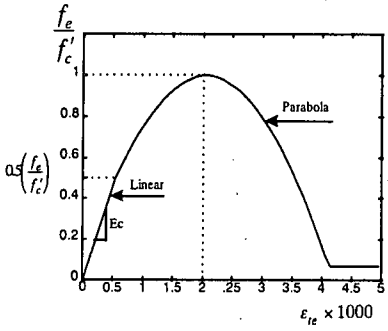

Fig. 2b Uniaxial concrete compression response

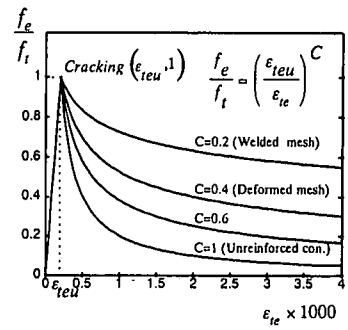

Fig. 2c Uniaxial concrete tensile response for various values of C

nodal displacement and $\mathbf{B}$ is the usual strain-displacement matrix. Once localization occurs, $\mathbf{B}$ matrix will be divided to two matrices $\overline{\mathbf{B}}_L$ and $\overline{\mathbf{B}}_N$ for two localized and nonlocalized regions respectively. Onset of localization takes place, strain increments are defined by

$$\Delta\boldsymbol{\varepsilon} = \mathbf{B}\Delta\mathbf{d} - \overline{\alpha}_N \mathbf{T} + L(s)\overline{\alpha}_L \mathbf{T} \tag{15}$$

where $\mathbf{T} = \hat{\mathbf{T}}/\|\hat{\mathbf{T}}\|$, $\overline{\alpha}_L$ and $\overline{\alpha}_N$ are magnitudes of the localized modes and $L(s)$ =1, 0 for localized and nonlocalized regions respectively. With respect to the **Fig.1**, the parameters $\overline{\alpha}_L$ and $\overline{\alpha}_N$ are determined by strain compatibility condition as

$$\overline{\alpha}_L = \frac{h}{b}\overline{\alpha}_N \tag{16}$$

where $\overline{\alpha}_L = \alpha_L \mathbf{T}^T \mathbf{B}\Delta\mathbf{d}$ and $\overline{\alpha}_N = \alpha_p \mathbf{T}^T \mathbf{B}\Delta\mathbf{d}$. With respect of Belytschko *et al.*[5], matrix $\overline{\mathbf{B}}$ is defined as

$$\overline{\mathbf{B}} = \begin{cases} \overline{\mathbf{B}}_L = (\mathbf{I} + \alpha_P (h/b - 1)\mathbf{T}\mathbf{T}^T)\mathbf{B} \\ \overline{\mathbf{B}}_N = (\mathbf{I} - \alpha_P \mathbf{T}\mathbf{T}^T)\mathbf{B} \end{cases} \tag{17}$$

and the strength of the jump mode

$$\alpha = \alpha_P (h/b)\mathbf{T}^T \mathbf{B}\Delta\mathbf{d} \tag{18}$$

where h is mesh size and can be calculated approximately by square root of element area A ($h = \sqrt{A}$) and α_P can be evaluated using equation 10. Detail of the procedure of calculation of α_P can be found in Belytschko *et al.*[5]. Once localization occurs, strain field will be divided to two localized and nonlocalized region so α_P will find an amount but varies in each step of load increments as well as displacement for every element. b is the shear bandwidth which is related to the fracture process zone of concrete and can be approximately identified from fracture tests for specimens of various geometries, in which the cracking is localized to a different extent. The crack bandwidth $b = 3d_a$ where d_a = maximum aggregate size, is approximately optimal[13]. Since h is not constant and varies in terms of element area so $\frac{h}{b}$ is related to the element area or size h.

As mentioned, one of the best advantage of the embedded method is that the bandwidth of localized region is independent to the element size. The intrinsic bandwidth b is introduced as a constitutive property of the band rather than as a geometric feature of the finite element mesh. Alternatively, in the discontinuity element a length scale parameter is introduced which is a material parameter and can be related to the size of the fracture process zone. This solves the mesh-size dependence problem present when a standard crack model is used.

4. CONSTITUTIVE MODELS

In this paper, for elasto-plastic calculation, the Drucker-Prager criterion which is modified to fit for concrete material is adopted. In the case of plane stress, the constants of the Drucker-Prager criterion are so determined in this analysis that the failure surface of the Drucker-Prager can go through the uniaxial tensile strength f_t and uniaxial compressive strength f_c' of concrete. In the case of compression in the failure surface, there will be a cut off to avoid more stress than f_c' **(Fig.2a)** in the analysis.

(1) Constitutive model of reinforcement

The behavior of reinforced concrete has been considered as the superposition of a material model for plain concrete and a material model for

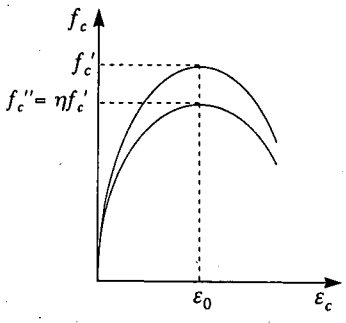

Fig. 3 Effect of tensil stress in concrete compressive respons

reinforcement. The material models for plain concrete will be presented in the next parts. The constitutive model of the reinforcement is assumed to be given by an elasto-plastic model with a linear elastic stiffness by

$$\mathbf{D}_s = \begin{bmatrix} \rho_x E_s & 0 & 0 \\ 0 & \rho_y E_s & 0 \\ 0 & 0 & 0 \end{bmatrix} \qquad (19)$$

in which ρ_x and ρ_y the reinforcement ratios in the X and Y directions respectively and E_s the Young's modulus of the reinforcement. The shear stiffness of the reinforcement is assumed to be equal to zero. After reaching the uniaxial tensile strength of f_{yt} or uniaxial compressive strength of f_{yc} in the reinforcement, related items in the stiffness matrix set by zero.

(2) Concrete compressive response in effective stress and effective strain form

The stress-strain curve of standard concrete cylinder subjected to a uniaxial compression is usually expressed mathematically by a parabolic curve:

$$\sigma_e = f_c' \left[2\left(\frac{\varepsilon_{te}}{\varepsilon_0}\right) - \left(\frac{\varepsilon_{te}}{\varepsilon_0}\right)^2 \right] \qquad (20)$$

where ε_0 is the strain at the peak stress f_c' and is usually taken as 0.002. The concrete compressive response in this paper is a parabolic curve with the initial linear part up to 50% of f_c' (**Fig.2b**). In the perfect parabolic model which has been frequently used by researchers, E_0, the initial tangential modulus, is $2f_c'/\varepsilon_0$ but in this model it is the same as E_c shown in **Fig.2b**. Small changes are proposed to allow better modeling and also to be adjusted with linear part of model.

In the compressive-compressive zone in the yielding surface (**Fig.2a**), two straight lines that go through f_c'' are adopted as the initial failure lines. These two lines are adopted while the stress state is in compressive-tensile condition otherwise in compressive-compressive condition, f_c' is used for concrete compressive strength instead of f_c'' for this case. The strength f_c'' is the compressive strength when the tensile strain ε_{te}, which is perpendicular to the compressive direction, is taken into account and can be evaluated by the equation. $f_c''= \eta f_c'$ where

$$\eta = \frac{1}{0.8 - 0.34(\varepsilon_{te} / \varepsilon_0)} \qquad (21)$$

and ε_0 is the strain at the peak stress f_c'. The maximum failure surface when the concrete is untouched can be shown in **Fig.2a**. After the material enter the plastic state, the failure surface at the first is increased up to the peak point (f_c') and then will be decreased according to the assumed uniaxial stress-strain curve.

(3) Concrete tensile response in effective stress and effective strain form

In describing the uniaxial stress-strain behavior of concrete, the model proposed by Okamura and Maekawa [8] is used after some modifications in this paper (**Fig.2c**). These modifications are introduced in order to increase the model efficiency while reinforcement is not presented in the element or distribution of the steel is not so good. Also, based on other research works like Gopalaratnam and Shah [9], horizontal part of the model has been eliminated. These modifications are in view of the fact that the response of typical reinforced concrete structure is much more affected by the tensile than by the compressive behavior of concrete. This stems from the fact that the concrete tensile strength is generally less than 20% of the compressive strength. In a typical reinforced concrete beam subjected to bending, the maximum compressive strength at failure does not reach a small fraction of the compressive strength at failure. Crack formation and propagation as well as yielding of the reinforcing steel therefore, dominate the behavior of these types of members.

A result of taking this approach is that the proposed concrete tensile response must now reflect the influence of the amount, distribution, orientation and type of the reinforcement. If the concrete is un-reinforced, then the average tension in the concrete

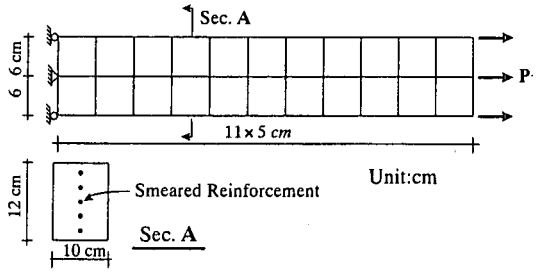

Fig. 4 FEM mesh and detail of specimen

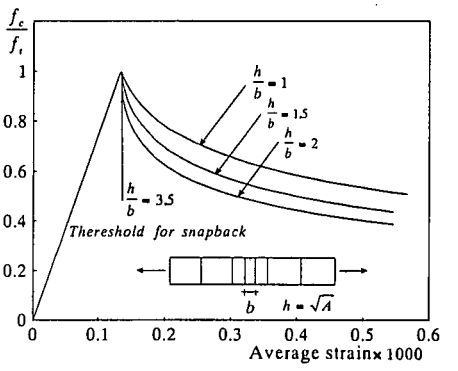

Fig. 5 Effect of bandwidth in tensile response

must reduce rapidly to zero. In this approach, it will not be zero but after sharp dropping, in this model it will go toward zero with a smooth curve (**Fig.2c**).

This is consistent with the experimental results of Gopalaratnam and Shah[9] who showed that even for unreinforced concrete, the tension in the concrete does not drop abruptly to zero, but that such mechanisms as aggregate and crystal interaction across the cracks cause significant post cracking strength. At the other extreme, if a large amount of well distributed reinforced is presented, then the considerable average tension should remain in concrete after cracking as has been observed.

Fig.2c shows used tensile stress-strain curve of concrete. The curves consist of two distinct branches. Before cracking the stress-strain relationship is essentially linear. Upon cracking however a drastic drop of strength occurs and the descending branch of the curve becomes concave. For well distribution of reinforcement in elements like shear walls or reinforced concrete panels, *C=0.4* gives reasonable results but for concentrated bars like reinforced concrete beams, the authors suggest *C=0.6* for this kind of structures. As shown in the **Fig.3b**, stress drops faster in the case of *C=0.6* than *C=0.4*. This is because of good distribution of reinforcement in *C=0.4* and in the one, reinforcements are not presented in every element.

5. NUMERICAL INVESTIGATION OF THE FEATURISTIC CHARACTER OF STRAIN JUMP

The constitutive models described and also mathematical expression is implemented into the finite element formulation in this section. All of the samples are subjected to monotonic loading. For the finite element solution, one point quadrature integration with hourglass control has been used in this program.

(1) Uniaxial loading

In this section, the model under uniaxial loading to obtain the effects of the localized bandwidth and reinforcement amount is scrutinized. For this case, the normal vector to the crack plan **n** is aligned with vector **m** i.e. $\mathbf{n}^T = \mathbf{m}^T = (1,0)$. **Fig.4** shows the finite element mesh and the specimen property under tensile loading and follows the stress-strain curve of **Fig.2c** with a fixed *C* value equal to 0.4. All reinforcing steel was treated as smeared.

a) Effects of bandwidth

For plain concrete, the effect of localized bandwidth to the assumed stress-strain relationship is shown in the **Fig.5**. As can be seen in this figure, softening behavior of the specimen will be increased as much as $\frac{b}{h}$ (or bandwidth of localized zone) reduced. This reduction is continued upon a threshold value of the $\frac{b}{h} = \frac{E_t}{E_t + E_c}$ where E_c and E_t are elastic and tangent modulus of concrete respectively (if the specimen considered as a one dimension system). In this case a sudden stress drop happens in the constitutive model and results a brittle fracture in the specimen. After this point, however snap back happens when $\frac{b}{h} < \frac{E_t}{E_t + E_c}$ and analysis will not converged if we use conventional displacement control algorithm. For this special case which is $E_t = -0.4E_c$ in the peak point of the tress-strain curve, the critical amount of the ratio for $\frac{b}{h}$ to snap back takes place is $\frac{b}{h} = \frac{1}{3.5}$.

b) Effects of reinforcement in the localization

The behavior of plane concrete in localization point of view is entirely different from the behavior of reinforced concrete. In the plain concrete, onset of reaching the peak point, independent of the

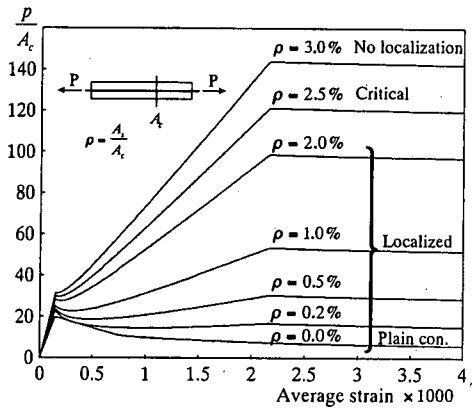

Fig. 6 Effect of steel ratio on localization in tension

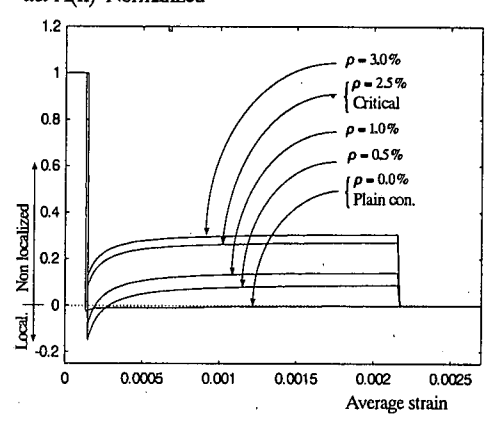

Fig. 7 Variation of *det* A(n) versus average strain

descending branch, localization happens due to softening behavior of the concrete. But in reinforced concrete due to the hardening behavior of the steel and softening behavior of the concrete, it is clear that the amount of the reinforcement has a key role to prevent or cause localized zone in the element. Moreover the amount of the steel, descending branch of the constitutive model for plane concrete as well as the hardening branch of the constitutive model of steel should be taken into the account.

The effects of the steel have been demonstrated in the **Fig.6**. As seen in figure, with ρ less than a critical value of $(-\frac{E_t}{E_s})$ and $\frac{1}{1-\upsilon^2}(-\frac{E_t}{E_s})$ in one and two dimension system where ρ, percentage of the steel and υ, Poisson's ratio, localization takes place in the specimen. These critical values are based on determinant of acoustic tensor which *det* **A(n)**=*0* has been calculated. It means that in **Fig.6** for $\rho \le 2.5\%$, *det* **A(n)** passes zero point while for $\rho > 2.5\%$, *det* **A(n)** is always positive. For two dimension system

$$\mathbf{A} = \begin{bmatrix} \frac{E_t}{1-\upsilon^2} + \rho E_s & 0 \\ 0 & \frac{E_c}{2(1+\upsilon)} \end{bmatrix}, \hat{\mathbf{T}} = \begin{Bmatrix} 1 \\ 0 \\ 0 \end{Bmatrix} \qquad (22)$$

where $\rho = \frac{A_s}{A_c}$, $\mathbf{m}^T = \{1,0\}$ and $\mathbf{n}^T = \{1,0\}$ which *det* **A(n)**=0 yields $\rho \le \frac{1}{1-\upsilon^2}(-\frac{E_t}{E_s})$ for localization condition. It is notable that the difference between cracking and localization is that crack in concrete occurs when principal tensile stress goes beyond f_t

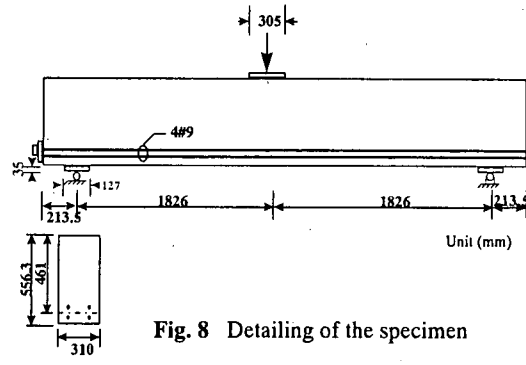

Fig. 8 Detailing of the specimen

but localization occurs after cracking when *det* **A(n)**=0 so in the case of no localization in **Fig.6**, concrete is cracked while *det* **A(n)**>0 hence in spite of cracking in concrete, due to the effect of reinforcement, localization does not occur.

The variation of *det* **A(n)** curve, as an indicator of the localization, versus loading stages has been shown in **Fig.7**. This figure shows how *det* **A(n)** varies in terms of average strain for a composite material such a reinforced concrete element. In the first part of the curves, materials are in the elastic state then localization indicator is positive and constant. On set of reaching to the peak point, there will be a drop and regarding to the amount of the steel, it can be localized or not.

(2) Beams subjected to bending and shear

In this part, two reinforced concrete beams, with and without web reinforcement have been analyzed and compared with experiment results. The beams have both failed in shear as reported. Half of the beams were modeled to reduce the time of calculation. The loads and the support reactions were both applied as distributed forces and

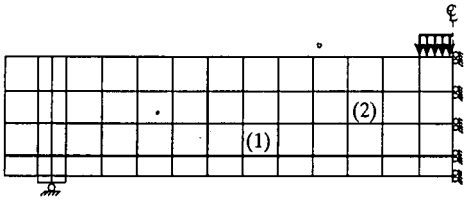

Fig. 9 Finite element mesh

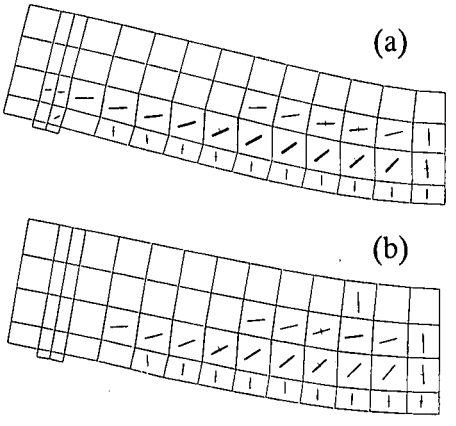

Fig. 10 Deflected shape and crack patterns in two cases a) Nonlocalized analysis and b) Localized analysis ($\times 20$). Unloaded elements at last stages have been indicated by a cross perpendicular to the cracks direction.

additional elements with stiffer properties have been used to avoid stress concentrations in the elements.

a) Beam tested by Bresler and Scordelis

Bresler and Scordelis [10] tested a series of beams in 1961 as part of a study on the shear strength of reinforced concrete beams. Beam OA-1 is analyzed here. The beam, shown in **Fig.8**, is heavily reinforced longitudinally to minimize the possibly of a flexural failure. There is no web reinforcement for this beam and the concrete must carry all of the shear stress. The finite element mesh used is shown in **Fig.9**.

The experimental load-deflection curve, together with the prediction from analysis in two cases of with and without localization effects are shown in **Fig.11**. The agreement with experimental results is very good in the case of localized calculation. As shown in **Figs.10(a)** and **10(b)**, in the case of nonlocalized analysis, despite the amount of the steel, it seems that beam is going to fail in flexural mode rather than in shear. As mentioned, in the overall behavior of the structures, localization, as a bifurcation phenomenon usually happens near to the peak point of loading as can be seen in **Fig.11**. In

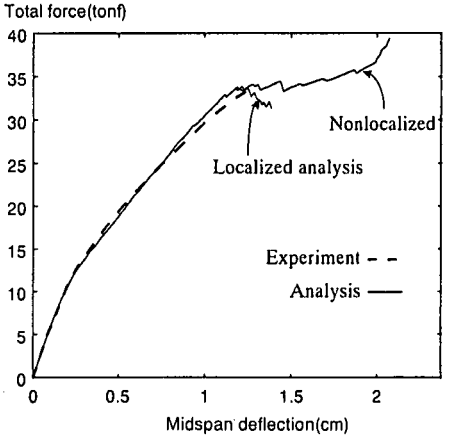

Fig. 11 Load versus midspan deflection

this figure, localized calculation shows softer behavior than in the second one and after bifurcation point, load will be decreased as much as deflection is increased due to going to the softening branch.

As reported by Bresler *et al.* diagonal tension failure occurred in this beam (beam OA-1). This beam and other beams which had no web reinforcement (OA-1, 2,3) failed shortly after the formation of the "critical diagonal tension crack". The failure occurred as a result of longitudinal splitting in the compression zone near to the load point. It is interested that the only crack, which formed in compression zone near to the loading point, is belong to the localized analysis (**Fig.10**). It is notable that the crack direction and also propagation are directly defined by equations (8) and (9) and their width (cracks) are based on plastic strains which are plotted to scale with respect to the displacement. Because the program used a smeared crack approach, the crack locations are arbitrary and form in gaussian points.

To contact this phenomenon in the element level, elements (1) and (2) have been considered in detail. The histories of effective plastic strain for both standard finite element method and proposed formulation are given in **Fig.12**. During the initial linear elastic deformation, the entire strains field is almost the same. During subsequent deformation, the strain in the conventional finite element grows proportionally. However at the onset of localization, the localized and nonlocalized strain take on different values. The nonlocalized strain gradually decreases, resulting in elastic unloading in the nonlocalized region, while the localized strain intensifies. These figures also show that the most plastic strain happens near to the peak point of loading in both cases of analysis. Moreover both

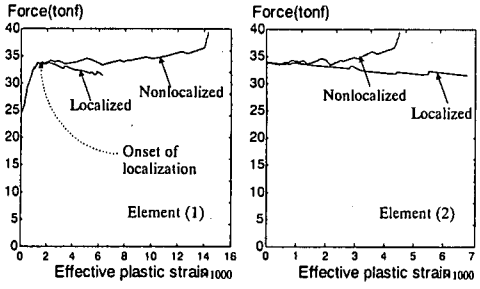

Fig. 12 Load versus effective plastic strain for the elements (1) and (2)

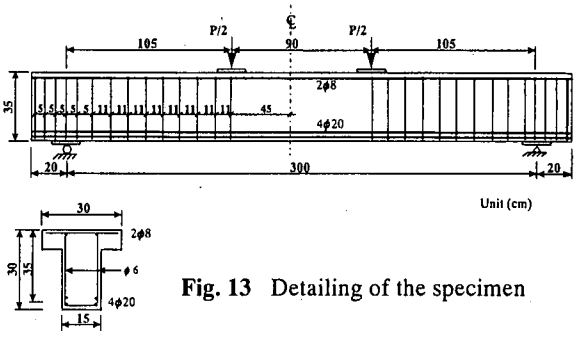

Fig. 13 Detailing of the specimen

elements (1) and (2) show softer behavior against loading as was also shown in the uniaxial case. In spite of the localized mode which plastic strains are near to each other in the both elements in nonlocalized analysis, plastic strains are considerably different than each other. This figure also implies different distribution of plastic strain in the elements.

To define mode of failure for these two elements, localization vector **n** and vector **m** can be found by the Eq. 8 which $\mathbf{n}^T.\mathbf{m}$ gives type of failure. For element (1) we have:

$$\mathbf{m} = \begin{Bmatrix} 0.927 \\ 0.375 \end{Bmatrix}, \quad \mathbf{n} = \begin{Bmatrix} 0.515 \\ -0.857 \end{Bmatrix} \qquad \mathbf{n}^T.\mathbf{m} = 0.156$$

which gives the angle of **n** and **m** equal to 81 degree is very near to pure mode II of failure (shear failure). It means this element fails in shear as can be seen in **Fig.10b**. For element (2) also we have:

$$\mathbf{m} = \begin{Bmatrix} 0.940 \\ -0.342 \end{Bmatrix}, \quad \mathbf{n} = \begin{Bmatrix} 0.105 \\ -0.995 \end{Bmatrix} \qquad \mathbf{n}^T.\mathbf{m} = 0.439$$

which gives the angle of **n** and **m** equal to 64.3 degree shows a mixed mode of failure in this element. As mentioned, when vector **m** is perpendicular to vector **n**, it shows pure mode II and when **m** is aligned with **n**, it is pure mode I of failure. Between this two amount, failure is in mixed mode (vectors **m** and **n** directions are based on **Fig.1**).

b) Analysis of simple supported beams with web reinforcement

A T-beam with web reinforcement which has been tested by Leonhardt and Walther[11] is analyzed here. The beam, shown in **Fig.13**, was supported on a span of 300 cm. The overall length of beam is 340cm and reinforcing steels are along the overall length of the beam without any hook or mechanical anchorage. The bearing lengths at the load points were 30cm by 12cm and at the reactions were 10cm by 15cm. The beam geometry and material properties are shown in **Fig.13**, along with the finite element mesh used to model the beam.

In this model, tension reinforcements have been considered as a one layer and all of the web reinforcing steel was treated as smeared and was included in the material properties of the reinforced concrete elements. The beam is heavily reinforced longitudinally in the tension zone and slightly reinforced by stirrups in the length of between loads and supports upon end of the beam. Shear failure at the compression zone near the loading point has been reported for this beam.

Fig.15 shows the deflected shape and crack patterns for the beam in two stages of loading for non localized calculation and final stage for localized calculation. The displacements and crack width are magnified by factors of 20 and 80 respectively. As mentioned earlier, the cracks are oriented with the shear band direction which can be determined by equations 5 and 8 in section 3.

The experimental load-deflection curve, together with the prediction from analysis in two cases of with and without localization effects are shown in **Fig.16**. Agreement with experiment results is good in the case of localized calculation comparing with conventional finite element analysis. It seems that if in these examples, we considered bond slip between steel and concrete, the results were much more closer to the experiment [12]. As shown in **Fig.16**, in the case of nonlocalized analysis, beam failed in higher load and deflection and mode of failure, due to the horizontal part of response, is near to flexural mode rather than shear. As mentioned in the previous example, in overall behavior of the structure, localization usually happens near to the peak point of loading as can be seen in **Fig.16** too. In this figure, in the localized response, onset of starting the softer branch, beam fails suddenly due to shear failure in some elements which shown in **Fig.15c**.

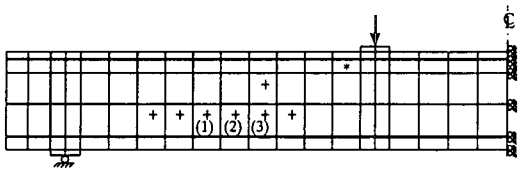

Fig. 14 Finite element mesh

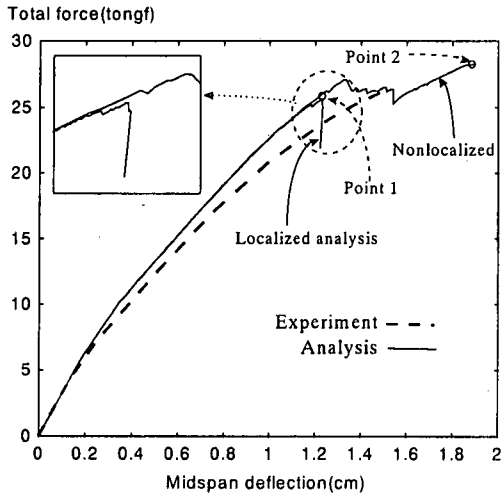

Fig. 16 Load versus midspan deflection

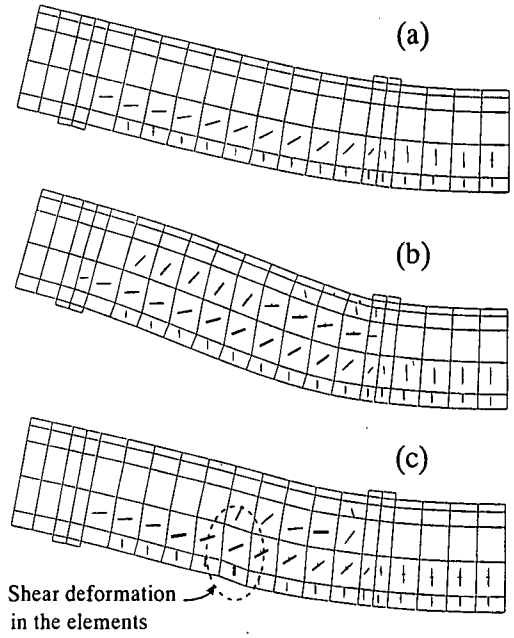

Fig. 15 Deflected shape and crack patterns in two cases: (a) and (b) Nonlocalized analysis at the point of (1) and (2) respectively and (c) is Localized analysis (× 20) at the point of (1). Unloaded elements at last stages have been indicated by a cross perpendicular to the cracks direction.

Because of the effect of web reinforcement, the softening branch is not extended as it was in beam without stirrups. This shows that the reinforcement does not let to softening branch formed clearly in the overall behavior of the beam but due to forming the shear band, response of beam is nearer to the experiment and beam fails in lower amount of loading and deflection.

Figures 17 and **18** show the histories of effective plastic strain for both conventional finite element method and proposed formulation in the elements (1) and (3) and also histories of shear strain in the element (2). During the initial linear elastic deformation, the entire strains field is almost the same. After shear band forming, the localized and the localized strain intensifies. Deformed shape of element (2) also can be seen in **Fig.15c** clearly. The mode of failure can be determined through vectors $\mathbf{m}$ and $\mathbf{n}$ where $\mathbf{n}^T\mathbf{m}$ gives type of failure. For foregoing elements:

Element (1): $\mathbf{n}^T.\mathbf{m} = 0.367$

Element (2): $\mathbf{n}^T.\mathbf{m} = 0.346$

Element (3): $\mathbf{n}^T.\mathbf{m} = 0.225$

which have good agreement with shear failure. In the elements (+) in the **Fig.14**, web reinforcements are yielded at the peak point of loading. Yielding process of stirrups is started from element (2) at the peak point and in next step, all other elements are yielded together and in this step, beam also failed.

As reported by experiment diagonal shear failure at the compression zone near the loading point has been occurred in this beam. In both cases of the analyses, diagonal cracks have been extended to compression zone but due to the higher amount of the load in non-localized analysis, compression crack is wider and more serious (**Figs.15b, c**). For better comparison between two cases, **Figs.15a** and **c** show crack patterns in non-localized and localized analyses which load level is the same as localized analysis (peak point of loading in the localized case). It is seen that there is no crack in compression zone in nonlocalized analysis as it is in localized one (element * in **Fig.14**). This shows better prediction of deformed shape and crack patterns of the method.

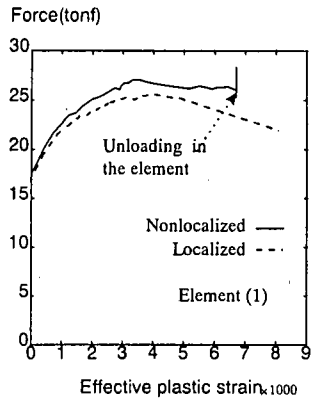

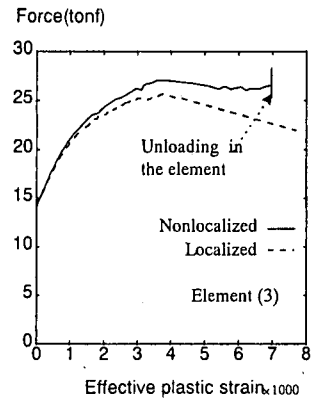

Fig. 17 Load versus effective plastic strain for the elements (1) and (3)

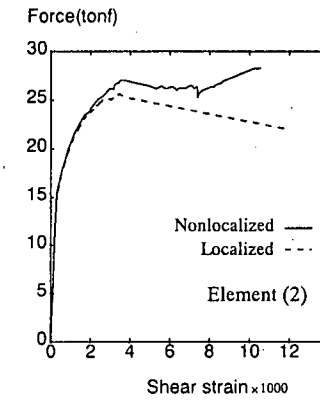

Fig. 18 Load versus shear strain for the elements (2)

6. CONCLUSION

In this paper, smeared crack model with embedded localized shear band has been developed and used for reinforced concrete members. The main purpose of this paper is to consider localization phenomenon in reinforced concrete beams which failed in shear. The principal of calculation is based on theory of plasticity with modified Draker-Prager criterion with compression cut off for yielding surface. The softening behaviors of concrete in both tension and compression have been expressed in the form of uniaxial stress-strain relationship with effective stress and effective strain regarding to the effective stress in Draker-Prager criterion.

The phenomenon of strain localization, which occurs in the material such as concrete, has been simulated into the finite element method. The base of this study is the finite element formulation for embedded localization zones proposed by Belytschko *et al.*[5] which was developed and used for reinforced concrete elements. For reinforced concrete as a composite material, mechanically, this phenomenon explained as a result of composite material instability when the composite material acoustic tensor losses its positive definiteness. The main purpose of this formulation is to define **B** matrix in finite element calculation onset of localization happens in an element. Through this theory, we can formulate strain discontinuity that usually observed in RC elements failed in shear.

Localization in material usually takes place in a narrow band which the bandwidth is related to the material property rather than mesh size. This can solves the mesh-size dependent problem with an acceptable accuracy. In numerical investigation, the adoption of the localization theory can effectively explains uniaxial fracture of concrete with or without reinforcement. It is shown that considering localization phenomenon in calculation causes much more softening in stress strain relationship.

After a threshold amount of shear bandwidth, snapback happens and the convergence cannot be obtained by conventional FE formulation. For reinforced concrete, in the case of uniaxial loading, the effects of steel based on Eq.9 also have been considered in detail. In this case, although localization occurs through Eq.9 when steel percentage is less than a special amount (critical amount) but in fact the effects of this phenomenon are much more important in slightly reinforced elements (**Fig.6**).

The application of the theory for two dimension elements (reinforced concrete beams) in plane stress condition has also been tried. The examples were two beams subjected to the monotonic loading and have failed in shear as reported. The results of analysis considering localization effects had better agreement with experiment than standard FE formulation. This effect was much clear in the beam without stirrups. Regarding to the differences between experiment and calculation results in two examples, it seems that if the effect of more reasonable bond had been considered in our model[12], the results would be much more nearer to the experiment results specially between first crack occurring and peak point of loading.

APPENDIX A SOLUTION OF THE LOCALIZATION CONDITION

Localization matrix A(**n**) for two dimension case is 2×2 and can be calculated as follow

$$det(\mathbf{A}(\mathbf{n})) = a_0 n_1^4 + a_1 n_1^3 n_2 + a_2 n_1^2 n_2^2 + a_3 n_1 n_2^3 + a_4 n_2^4 \quad (A.1)$$

where

$$a_0 = D_{1111}D_{1212} - D_{1112}D_{1211},$$

$$a_1 = D_{1111}D_{1222} + D_{1111}D_{2212} - D_{1112}D_{2211} - D_{1122}D_{1211},$$

$$a_2 = D_{1111}D_{2222} + D_{1112}D_{1222} + D_{1211}D_{2212} - D_{1122}D_{1212} - D_{1122}D_{2211} - D_{1212}D_{2211},$$

$$a_3 = D_{1112}D_{2222} + D_{1211}D_{2222} - D_{1122}D_{2212} - D_{1222}D_{2211},$$

$$a_4 = D_{1212}D_{2222} - D_{2212}D_{1222} \quad (A.2)$$

It is notable that D in this formulation is tangential constitutive matrix for composite material of reinforced concrete element which can be obtain by Eq. 14 in section 2. Setting $n_1 = \cos\theta, n_2 = \sin\theta$ in (A.1) the localization condition becomes

$$f(x) = a_4 x^4 + a_3 x^3 + a_2 x^2 + a_1 x + a_0 x \quad (A.3)$$

where $x = \tan\theta$. In general, the polynomial $f(x)$ in (A.3) is positive everywhere prior to localization. Thus the onset of localization can be determined by simply examination the sign of the minima of $f(x)$. These occur at the roots of the cubic polynomial $f'(x)$ which can be computed in close form by means of Cardon's formulae. As long as the minima of $f(x)$ remain positive localization does not develop. The onset of localization is signaled by one or more minima of $f(x)$ crossing the x-axis.

REFERENCES

1) Tanabe, T., Yu, G. and Salamy, M.R.: Analysis of the localized failure phenomenon in reinforced concrete shear walls, Conference on comp. modeling of concrete structures, Badgastein, Austria, pp. 265-274, 31 March-3 April 1998.
2) An, X. and Maekawa, K.: Size effect for shear strength of reinforced concrete, Proc. of JCI, Vol. 18, No. 2, pp. 635-639, 1996
3) Hill, R.: Acceleration waves in solids, J. Mech. Phys. Solids, Vol. 10, pp. 1-16, 1962.
4) Ortiz, M., Leory, Y. and Needlemann, A.: A finite element method for localized failure analysis, J. Comput. Meths. In Appl. and Mech. Engrg., 61, pp.189-214, 1987.
5) Belytschko, T., Fish, J. and Engelmann, E.: A finite element with embedded localization zones, J. Comput. Meths. In Appl. and Mech. Engrg., 70, pp. 59-89, 1988.
6) Tanabe, T. and Yoshikawa, H.: Constitutive equations of a reinforced concrete panel. IABSE, Col., Delft 1987.
7) Dahlblom, O. and Ottosen, N.S.: Smeared crack analysis using generalized fictitious model, J. Engrg. Mech. Div., ASCE, Vol. 116, No. 1, pp. 55-76, 1990
8) Okamura, H. and Makekawa, K.: Nonlinear Analysis and Constitutive Models of Reinforced Concrete., pp. 28-60, 1991.
9) Gopalaratnam, V. S. and Shah, S. P.: Softening response of plain concrete in direct tension, J. ACI, Proceeding V. 82, No. 3, pp. 310-323, May-June 1985.
10) Bresler, B. and Scordelis, A. C.: Shear strength of reinforced concrete beams, J. ACI ,*Proceeding V.* 60, No. 1, pp. 51-72, Jan. 1963.
11) Leonhardt, F. and Walther, R.: Beitrage zur behandlung der schubprobleme im stahlbetonbau, J. BETON-UND STAHLBETONBAU, 1962. 7. Heft 7, pp. 161-173.
12) Kwak, H. G. and Filippou, F. C.: Nonlinear FE analysis of RC structures under monotonic loads, J. Computer and Structures, Vol. 65, No. 1, pp. 1-16, 1997.
13) Bazant, Z. P. and Planes J.: Fracture and Size Effect in Concrete and Other Quasibrittle Materials., pp. 227, 1998.

(Received April 12, 1999)

局所化破壊を考慮したRCはりのせん断破壊解析

Mohammad Reza SALAMY・余　国雄・田辺　忠顕

本研究においては，鉄筋コンクリートの1次元部材（軸引張，或いは軸圧縮部材），或いは2次元部材（はり，或いは壁部材）の局所化破壊，特に2次元部材のせん断破壊について，材料レベル構成則のAcoustic Tensorの固有値解析から導かれる分岐枝と破壊との関連を詳細に検討した．その結果，RCはりのせん断破壊現象ならびにひずみの発生状況などの現象の説明がより合理的に行えることが判明した．